# *Hibiscus sabdariffa L.* calyces' and argon DBD plasma: potential eco-friendly cleaners for fire-damaged silver gelatin prints

*Laila M. Elattar and Sawsan S. Darwish*
Conservation Department, Faculty of Archaeology, Cairo University, Giza, Egypt
*Usama M. Rashed*
Physics Department, Faculty of Science, Al-Azhar University, Cairo, Egypt
*Maha Ahmed Ali*
Conservation Department, Faculty of Archaeology, Cairo University, Giza, Egypt, and
*Shaimaa M. Eldeighdye*
Nuclear Research Center – Biological Applications Department, Egyptian Atomic Energy Authority, Cairo, Egypt

**Abstract**

**Purpose** – This paper aims at examining the potentiality of using *Hibiscus sabdariffa L.* calyces' (Hs) aqueous extract to remove soot stains from the surface of fire-damaged silver gelatin prints. It further studies the cleaning efficiency and impact of both a contact method and a noncontact method with argon dielectric barrier discharge plasma (DBD Ar. plasma) on the different properties of silver gelatin prints. Accordingly, it prompts using economic, eco-friendly materials and methods in the photograph conservation field.

**Design/methodology/approach** – To achieve the aims of this paper, four silver gelatin prints were stained with soot and treated with the Hs aqueous extract as a contact method and DBD Ar. plasma combined with the aqueous extract as a noncontact method. The assessment was carried out using digital microscopy, atomic force microscopy and spectrophotometer to study the efficiency of the tested treatments and their impact on the surface of the photographs. Fourier transform infrared was used to monitor the state of the binder after cleaning. Furthermore, the pH and the mechanical properties were measured.

**Findings** – The contact method resulted in lower concentrations of Hs extract that efficiently cleaned the surface without causing any stains or damage to the treated photographs. The noncontact method (plasma with an aqueous extract) proved to be less effective in cleaning and made the binder more susceptible to deterioration.

**Originality/value** – This paper reveals the success of Hs aqueous extract in cleaning soot on vulnerable photographs' surfaces.

**Keywords** *Hibiscus sabdariffa*, Argon plasma, Eco-friendly cleaning, Silver gelatin prints, Soot stains

**Paper type** Research paper

## 1. Introduction

Photographs of high historic, social and artistic value exist abundantly worldwide. These are of great significance as documentary tools reflecting the past and present (Zachariášová *et al.*, 2019; Ali *et al.*, 2017). In the 20th century, silver gelatin photographs were the most dominant photographic processes and were introduced in the 1880s (Sullivan, 2014; Sclocchi *et al.*, 2013). Silver gelatin prints were either printed out or developed out (DOP). DOP silver gelatin prints form an essential part of photographic collections since they exist in large numbers among archival collections of museums, libraries and archives worldwide (Tomšová and Ďurovič, 2017). A DOP silver gelatin print has a layered structure composed of three main layers (Oravec *et al.*, 2019): the paper support which physically supports the image layer, the photographic binder layer of gelatin and an opaque interlayer between the support and the final layer consisting of white pigment, barium sulfate, which is finely grounded in gelatin (Yosri *et al.*, 2020). Finally, the metallic silver: fine silver particles are dispersed in the gelatin binder forming the final image layer (Shaheen *et al.*, 2020; Abdel-Aziz *et al.*, 2019).

Throughout history, libraries, museums and archives have experienced fire hazards that are manmade or a result of a natural disaster (Superio *et al.*, 2019). Wildfire and lightning have destroyed some libraries (Nordling, 2021; Maher, 2018; Inklebarger, 2018). Moreover, human-induced fire (i.e. electrical equipment, arson and wars) has damaged several libraries (Gupta, 2019; Chawinga and Majawa, 2018). A fire that occurred at the Hale Library, KS University, USA, in 2018 caused the staining of the collections' surfaces with a film of soot as a result of the presence of smoke, water and high

The current issue and full text archive of this journal is available on Emerald Insight at: **https://www.emerald.com/insight/0369-9420.htm**

Pigment & Resin Technology
52/1 (2023) 91–104
 [ISSN 0369-9420]
[DOI 10.1108/PRT-07-2021-0085]

Received 5 August 2021
Revised 8 October 2021
Accepted 18 October 2021

temperature (Rebekah, 2018; Turvey-Welch and Talbot, 2018). During fires, the high relative humidity contributes to the expansion and softening of the gelatin binder layer, and the resultant soot adheres to the image surface of the silver gelatin prints. With humidity and heat fluctuations, the soot layer becomes more coherent to the surface and difficult to remove. Consequently, the main risk of soot is not restricted to the aesthetic aspects (Giacometti *et al.*, 2016) as it also causes inevitable physical and chemical deterioration.

Cleaning photographs using methods that do not negatively affect the microstructure of the object is quite a challenge. Cleaning, if not performed appropriately using proper materials and methods, may cause irreversible damage (Pianorsi *et al.*, 2017; Domingues *et al.*, 2013). Based on previous studies, mechanical/dry cleaning (i.e. erasers and brushes) may damage the image layer and the binder (Ali, 2016), and organic solvents treatments are not eco-friendly and alter the appearance of the object's surface and properties (Clarke *et al.*, 2018; Volpi, 2017). Therefore, there is a need to find a safe treatment that does not harm the environment, the conservator and the object to be treated. There are limited ecological cleaning methods to remove soot from artifacts (Al-Emam *et al.*, 2021). The novel alternative cleaning approaches that have been chosen to be examined in this study are *Hibiscus sabdariffa L.* (*H. sabdariffa L.*) calyces aqueous extract, separate and with argon dielectric barrier discharge plasma (DBD Ar. plasma).

*H. sabdariffa L.* calyces aqueous extract (Hs) is a sustainable solvent extracted from a natural material. It is a herb (family Malvaceae) commonly known as roselle, hibiscus and Karkade. This precious extract is cultivated in some tropical and subtropical areas (El-Kinany *et al.*, 2020). It is available in Middle Eastern countries, China, Thailand, Mexico, etc. (Izquierdo-Vega *et al.*, 2020). Egyptian roselle contains higher quantities of anthocyanins and sugars (Pinela *et al.*, 2019; Da-Costa-Rocha *et al.*, 2014). The Hs plant is popular for its applications in food, medicine, cosmetics and pharmaceutical industries (El-Kinany *et al.*, 2020; Naeem *et al.*, 2019). The most important part of Hs is calyx, which has high antimicrobial activities (Salami and Afolayan, 2020). The main chemical constituents of Hs calyces' aqueous extracts are anthocyanins, flavonoids, phenolic acids and a large percentage of organic acid (Jamini *et al.*, 2018), including hibiscus acid, hydroxycitric acids, citric acid, malic, as well as tartaric and minor compounds, oxalic acid and ascorbic acid. The number of components varies because of genetics, ecology and harvest circumstances (Da-Costa-Rocha *et al.*, 2014).

The presence of acids in a Hs aqueous extract may be harmful to photographs when using the contact method; accordingly, atmospheric plasma as a noncontact method is also investigated. Recent plasma treatments performed on photographs have shown no significant changes, and post-treatment has provided long-term stability for objects (Zachariášová *et al.*, 2019) improving the overall visual appearance (Boselli *et al.*, 2017). Plasma treatment is considered the eco-sustainable alternative treatment for the current cleaning methods (Grieten *et al.*, 2017). This method decreases the possible damage resulting from mechanical contact with a fragile material surface and can be precisely controlled. It is entirely a nontoxic, noninvasive procedure and greener than chemical processing (Ioanid *et al.*, 2016).

Chemical cleaning may leave residues on surfaces after cleaning. While, plasma cleaning generates energetic plasma components, ions, electrons and neutrals (atoms, molecules and radicals) from inherent gaseous species (i.e. argon and air) to remove both contaminants and invisible residues found on surfaces without leaving any residue (Tinõ *et al.*, 2019). The plasma cleaning mechanism is performed by the interaction between the discharge components (i.e. electrons, ions, photons and radicals) and soot – the first layer of the surface (El-Gohary and Metawa, 2016). Their interaction with the surface of the contamination causes mainly three basic processes that lead to surface cleaning: heating, sputtering and etching. Heating by plasma is mainly performed by electron and ion bombardment and by plasma radiation. Heating to moderate temperatures can remove only the physisorbed or lightly bonded contaminants. Sputtering is nonselective and not always a sufficiently effective cleaning process. It strongly depends on the nature of the surface and the type of contaminants. However, plasma cleaning by sputtering is widely carried out in various technological processes, where plasma etching and heating alone cannot provide the desired cleanness. In plasma cleaning by etching, atoms or radicals from the plasma chemically react with the surface. The choice of the plasma chemistry is determined by the volatility and stability of the etch products. Plasma cleaning is significantly enhanced when all or some of these three main processes are combined (Belkind and Gershman, 2008). Although atmospheric plasma decontamination has proven its success on a diverse range of substrates, it is still a novel technique in the research scope (Stefanova and Kamenarov, 2020).

In this study, Hs aqueous extract as a contact method and DBD argon plasma combined with absolute Hs aqueous extract as a noncontact method were investigated. The mixture of the DBD argon plasma with aqueous extract was used depending on the chemical etching process.

## 2. Materials and methods

### 2.1 Materials

#### *2.1.1 Silver gelatin prints*

A group of five non-valuable silver gelatin prints (DOP) dating back to 1946 was used in this study. Four photographs were numbered as follows: FI, F2, F3 and F4. The size of each photograph ranged between 12 and 13 cm long and 8.9 cm wide. These were assigned to the contact method. The photograph assigned to the noncontact method was numbered S and was 25 cm long and 25 cm wide (Figure 1).

#### *2.1.2 Hibiscus sabdariffa L. calyces*

Dried dark red *H. sabdariffa L.* calyces of 125 g were obtained from the agricultural research center, Giza, Egypt. The plant was harvested from Upper Egypt.

#### *2.1.3 Dielectric barrier discharge setup*

Figure 2 shows a schematic diagram of the DBD reactor used to clean the photographs from soot. It consisted of two parallel electrodes. The upper electrode was a circular disc of stainless steel with a diameter of 4 cm and a thickness of 1 cm attached to a glass disc (10 cm diameter and 1 mm thickness) by a circular rubber ring (O-ring) of 8.5 cm diameter and 3 mm thickness. The lower electrode was a stainless-steel plate of $25 \times 25$ $cm^2$ area.

**Figure 1** A for (F1) image; B from the right to the left for (F2, F3, F4) images; and C for (S) image


**Figure 2** Schematic diagram of the dielectric barrier reactor used for cleaning photographs from stains

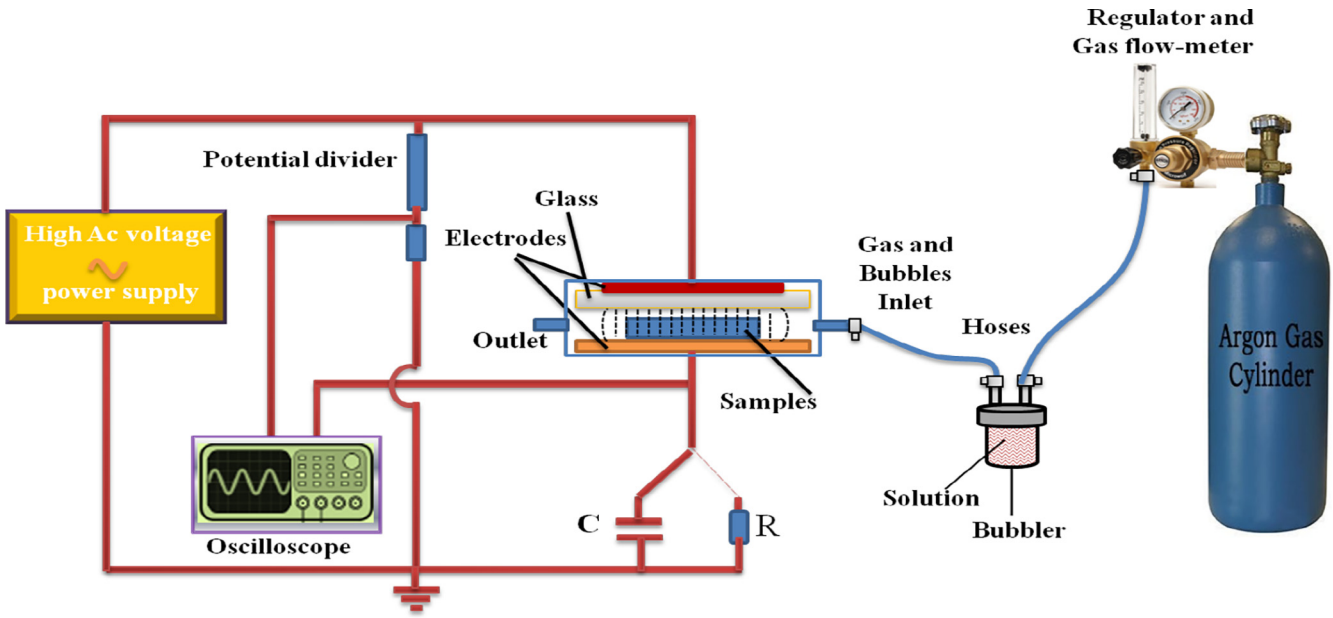


The gap distance between the glass disc and the lower electrode was 3 mm. Two ports were used as a gas inlet and outlet.

The plasma discharge was produced by a 25 kV/30 mA AC power supply source at a frequency of 50 Hz connected to the upper electrode, while the lower electrode was connected to the ground through a resistor R = 100 Ω or a capacitor C of 3.35 $\mu$F capacitance. Samples were placed in the gap between the two electrodes. The gas freely flowed through the gas flow meter to the bubbler then into the gap between the two electrodes where the electrical discharge was generated in this space. The working gas used for cleaning was argon at a flow rate of 3 L/min, and the solution used inside the bubbler was *H. sabdariffa* aqueous extract of absolute concentration. Plasma cleaning was performed with different exposure times and different applied voltages. The voltage across the discharge electrodes was measured using a high voltage probe (resistive voltage probe) connected parallel to the discharge electrodes. The discharge current was measured by measuring the voltage drop across the resistor R with a two-channel digital oscilloscope (GWinsTEX GDs-1072-u, 70 MHz). The charge transferred through a DBD reactor was measured by a capacitor 3.35 mF connected in series with the DBD reactor. The dissipated power during the discharge was estimated using the Lissajous figures method (Figure 2).

## 2.2 Methodologies

### *2.2.1 Preparation of soot stains*

*2.2.1.1 Contact method.* The surface of the photograph (F1) was already stained with candle wax and different commercial adhesives mixed with different types of soot (i.e. ash wood, candle flame and burning wood flame). This photograph was treated with all Hs aqueous extract concentrations to determine which one will not leave a stain on the surface. Each photograph (i.e. F2, F3 and F4) was assigned to be treated with the most appropriate concentrations and was divided into halves; one half was set as a control (unstained) sample, and the other half was stained with a burning wooden frame flame to simulate wildfires and the burning of frames and buildings [Figure 3(a) and (b)].

*2.2.1.2 Noncontact method.* Likewise, the photograph (S) was cut into two pieces: one for a control (unstained) sample and the other piece into smaller pieces measuring 2 cm × 2 cm and stained with the flame of the burning wooden frame. All stained pieces were then divided into four groups; each group was divided into three areas (i.e. shadow, mid-tone and highlight). These were assigned to four conditions (I, II, III and IV) of plasma with aqueous extract treatment.

All photographs were exposed to water vapor after staining to simulate the humidity in the site during fires and ensure that the

**Figure 3** Staining process: (a, b) applying the soot by exposing the surface to flame of the burning wood; (c) exposure of the photographs after staining to water vapor; and (d) F2, F3, F4 and S samples in ambient air for complete dryness after staining

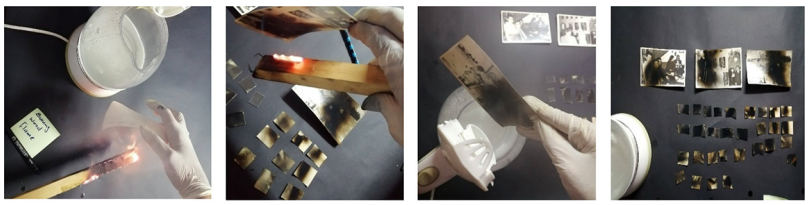

(a) (b) (c) (d)

soot was coherent with the surface of the photographs. The staining process was executed in 5 h at 96% RH; then, samples were left at room temperature for two days for complete dryness [Figure 3(c) and (d)].

*2.2.1.3 Artificial aging.* All stained samples were exposed to artificial aging at a temperature of 80°C ± 2°C and relative humidity of 65% for three days according to ISO standard 5630–3:1996 to expedite the age of stains and ensure their adhesion to the surfaces.

*2.2.2 Preparation of Hibiscus sabdariffa L. aqueous extract*

Aqueous extract of *H. sabdariffa* was selected for the experiments. Although aqueous cleaning may cause the gelatin binder to swell, causing cracking, pitting or even loss, it may be needed if the contaminant is embedded in the gelatin layer. Slight swelling is beneficial for easy removal (Ali *et al.*, 2017). Hs calyces of 125 g was washed with tap water to clean them from dust and then soaked in 1 L of distilled water in a glass bowl at room temperature ranging from 16 to 25°C for 48 h with continuous shaking. The aqueous extract was filtered using double rings 102 filter paper 12.5 cm paper No.1, and the residue was discarded. The resultant aqueous extract was used in different ratios, Hs aqueous extract to distilled water as follows: 7 ml:93 ml, 15 ml:85 ml, 25 ml:75 ml, 50 ml:50 ml, 70 ml:30 ml and the absolute.

*2.2.3 Treatment methods set as follows*

*2.2.3.1 Method I: contact method (Hs aqueous extract concentrations).* First, all concentrations were tested using a cotton swab on the F1 photograph to determine their suitability. Then, the most suitable concentrations were applied with cotton swabs on F2, F3 and F4.

*2.2.3.2 Method II: noncontact method (plasma and absolute of Hs aqueous extract)* This method was performed with argon gas at a flow rate of 3 L and Hs aqueous extract of absolute concentration in a bubbler. The samples were placed in the gap between the two electrodes. The gas freely flowed through the gas flow meter to the absolute aqueous extract inside the bubbler. The argon gas was saturated with the vapor of the solution and entered to the gap between the two electrodes where the electrical discharge was generated. Then the gas with the vapor was subjected to the electrical discharge, forming ions, electrons and other reactive species (Figure 4). The plasma cleaning process was performed by two mechanisms: first, enhanced dry chemical reaction (chemical etching) between these formed reactive species and stains producing volatile products that led to the cleaning process. This chemical etching was the most effective and strongest contribution to the cleaning process: second, physical sputter of ions, atoms and other plasma species which weakly contributed to the cleaning process. The treatment was implemented in different treatment periods (i.e. 10 and 20 min) and different power (i.e. 1.5 and 2.5 W) for four conditions: I: (10 min/1.5 W), II: (20 min/1.5 W), III: (10 min/2.5 W) and IV: (20 min/2.5 W). The treatment processes were initiated with low condition up to high Figure 4.

**Figure 4** Induced plasma during method II treatments

*2.2.4 Cleaning assessment*

*2.2.4.1 Digital microscope.* Visual inspection was carried out using a mobile digital microscope (5 MP sensor, a microscopic lens with 500 magnification and measurement of software (1/1,000 mm). It was used to examine the photographs' surface characteristics and any changes in the post-treatments.

*2.2.4.2 pH measurement.* The pH values were measured to detect any alteration in the acidity of the photographs after treatments using two tools: the pH paper strips (MColorpHast$^{TM}$) and the Adwa waterproof pH-Temp tester portable device. The first tool: a drop of water was placed on the surface by pipette; then, the pH paper strips were placed over it and left for a few minutes. After the color of the strip changed, it was compared with the standard pH value. Both tests were done for control samples and stained samples before and after treatments.

*2.2.4.3 Colorimetric measurement.* Color changes were measured using a MiniScan Model No. EZ MSEZ0693 to investigate any color alteration because of the treatments. The analysis conditions were as follows: in the visible region, i.e. a wavelength range from 400 to 700 nm, with an interval of 10 nm, using a D65 light source and 10° of observed angle. The CIE LAB color space system (CIE 1976) was used, where the color parameters ($L^*a^*b^*$) data were collected, $L^*$ corresponds to the brightness (100 = white, 0 = black), $a^*$ to the red-green

coordinate (positive sign = red, negative sign = green) and b* to the yellow-blue coordinate (positive sign = yellow, negative sign = blue) (Cattò *et al.*, 2021; Prieto *et al.*, 2020). The total color difference (ΔE*ab) was calculated using the equation: $\Delta E^* = \{(\Delta L^*)2 + (\Delta a^*)2 + (\Delta b^*)2\}^{1/2}$ (Lettieri *et al.*, 2021; Cattò *et al.*, 2021). The analysis was carried out at the Wood Conservation Laboratory, Faculty of Archaeology, Cairo University.

*2.2.4.4 Atomic force microscope.* One of the most popular analytical procedures used to evaluate the effectiveness of the cleaning process and detect residues on the cleaned materials' surface is atomic force microscopy (Hrdlickova Kuckova *et al.*, 2014). It is applicable to photograph (Nieto-Villena *et al.*, 2018). The atomic force microscope (AFM) used in this investigation was a Thermo Microscope Autoprobe CP – Research head model MLCT manufactured by Bruker operated in contact mode using a silicon nitride probe. The results were obtained in two dimension, three dimension images and histogram. The scan area was 20 × 20 $mm^2$, scan rate 1 Hz and resolution 256 × 256. The Proscan 1.8 software was used to control the scan parameters, the IP 2.1 software was used for image analysis, and the color scale was false. The analysis was performed at the National Institute for Standards, Giza, Egypt.

*2.2.4.5 Fourier transform infrared-attenuated total reflection analysis.* The Fourier transform infrared (FTIR) spectroscopy provides information on proteins' structural characterization and conformational changes (Adochitei and Drochioiu, 2011). The FTIR instrument used was Thermo Nicolet 380 under the transmission mode in the frequency range of 4.000–400 $cm^{-1}$ to study the gelatin binder after treatments. The analysis was done at the National Institute of Standards, Giza, Egypt.

*2.2.4.6 Mechanical properties.* Tensile strength and elongation percent were used to define the ultimate tensile force per unit width in the treated sample before rupture or refraction and the maximum stretching of the treated sample at the ultimate tensile force before rupture at stable conditions (Shaheen *et al.*, 2019). The measurements were conducted by H5KT130-500N/E139-34 A machine using a strip method according to ISO 13934–1;1999 at the National Institute for Standards (NIS), Giza, Egypt.

## 3. Results and discussion

### 3.1 Method I: contact method

Screening the suitability of Hs aqueous extract concentrations.

Figure 5 showed that visually all concentrations were effective in removing the hard coherent stains from the F1 photograph's surface. Each of the absolute, 70 ml:30 ml and 50 ml:50 ml, left a red stain post-treatment. Therefore, the other concentrations were decided to be used as they did not leave any stains on the photographs' surface; 7 ml for F2, 15 ml for F3 and 25 ml for F4.

The three concentrations of Hs (7, 15 and 25 ml) removed perfectly the soot stains as displayed in Figures 6-8.

### 3.2 Method II: noncontact method

After trying all the concentrations of the extract, the absolute was the one that provided a good result.

*3.2.1 Electrical characterization*

In Figure 9, it was noticed that several high-frequency peaks were superimposed at the maximum amplitude of the current

**Figure 5** F1 photograph: (a) before; (b) during; and (c) after treatment


(a) (b) (c)

**Figure 6** F2: (a) before, (b, c) during, (d) after treatment with 7 ml:93 ml of Hs aqueous extract

(a) (b) (c) (d)

**Figure 7** F3: (a) before, (b, c) during and (d) after treatment with 15 ml:85 ml of Hs aqueous extract

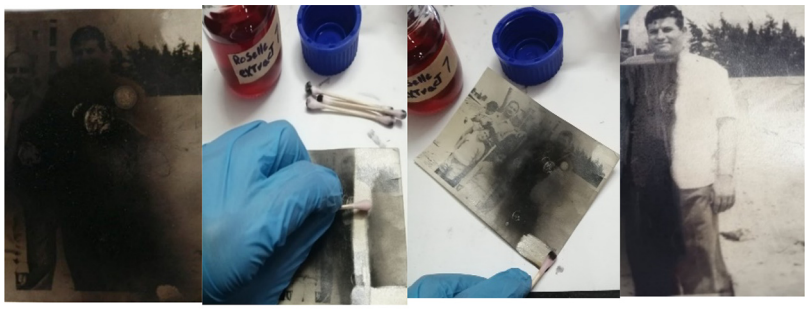


**Figure 8** F4: (a) before, (b–d) during and (e) after treatment with 25 ml:75 ml of Hs aqueous extract


**Figure 9** Waveforms of the voltage applied to the reactor and the associated discharge current applied voltage Vpp: (a) 18 kV and (b) 24 kV, respectively

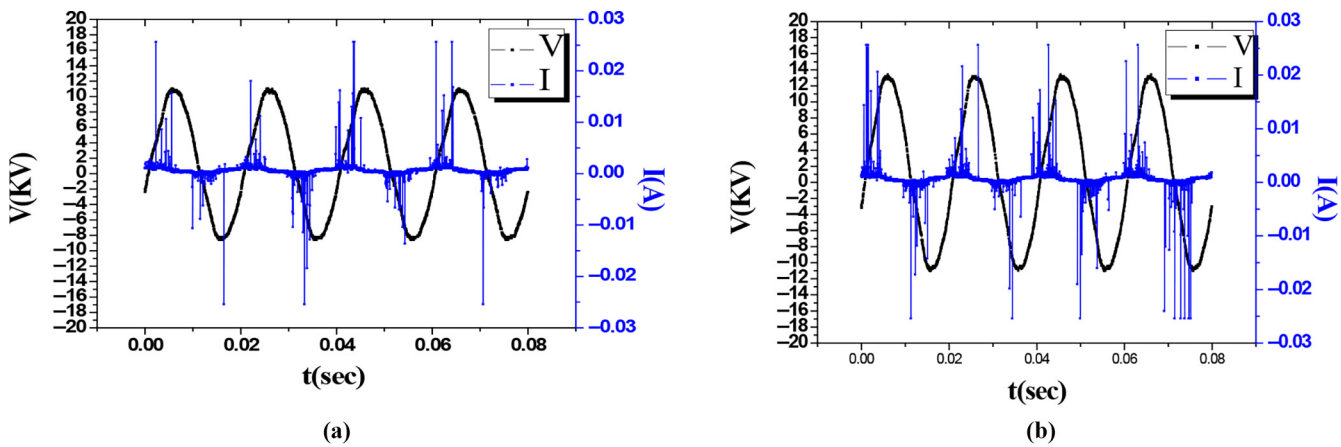


waveforms. The amplitude and the number of these peaks increased with the increase in applied voltage. The individual peaks were very narrow, corresponding to a short burning time of the individual filaments in the nanosecond range. This finding indicated that the discharge regime was filamentary. The filaments crossed the discharge gap and spread on the surface of the dielectric barrier, building up surface charges, which produced an electric field opposite to that of the applied voltage. So after a short time (several ns), the filament activity in that spot was turned off, followed by filament initiation in another location (Abdelghaffar *et al.*, 2020). The consumed power could be estimated simply by using the Lissajous (Figure 10). Lissajous figures were obtained by plotting the charge transferred during the discharge as a function of the applied voltage. The charge transferred through a DBD reactor was measured by a capacitor 3.35 $\mu$F connected in series with the DBD reactor. The result ideally was a parallelogram, whose area equaled the electrical energy during one discharge cycle. By multiplying the electrical energy with the frequency of the

**Figure 10** Lissajous figures of DBD reactor using argon gas (flow rate 3 L/min) at applied voltages Vpp: (a) 18 kV and (b) 24 kV, respectively (X-axis × 1.675 $\mu$F and Y axis × 5 kV)


(a) (b)

applied voltage, the consumed power during the discharge was calculated (Ahmed *et al.*, 2016).

The consumed power was calculated by multiplying the area of the parallelogram by the frequency of the used AC power supply (50 Hz) to be 1.5 and 2.5 W for applied voltages Vpp equal to 18 and 24 kV, respectively.

As displayed in Figure 11, stains were removed visually only in conditions III and IV, which was more efficient in cleaning.

### 3.3 Cleaning assessments

Digital microscope, spectrophotometer and pH measurements were implemented on all treatments; upon their results, AFM,

**Figure 11** Four conditions of method II before, after and unstained control samples

| Sample | Condition I (10 min – 1.5 W) | | Condition II (20 mins-1.5 W) | | Control |
|---|---|---|---|---|---|
| | Before | After | Before | After | |
| Shadow |  | 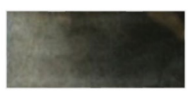 |  |  | 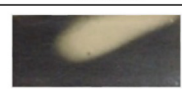 |
| Midtone |  | 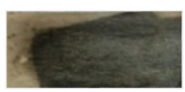 |  |  |  |
| Highlight | 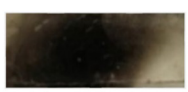 | 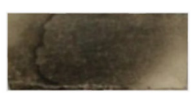 |  |  |  |
| Sample | Condition III (10 min – 2.5 W) | | Condition IV (20 min – 2.5 W) | | Control |
| | Before | After | Before | After | |
| Shadow |  |  |  |  |  |
| Midtone | 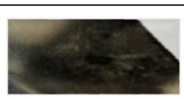 |  |  |  |  |
| Highlight |  |  |  |  |  |

FTIR and mechanical properties were carried out on the most effective treatments from each method.

*3.2.1 Digital microscope*

*3.2.1.1 Method I: contact method (Figure 12)*
*3.2.1.2 Method II: noncontact method (Figure 13)*. Each Figures 12 and 13 showed that visually, post-cleaning investigations revealed that the first method led to full cleaning for all concentrations, while the second method achieved partial cleaning in the III condition after 10 min. In the same context, the IV condition improved cleaning after 20 min leaving a light residue of soot.

*3.2.2 pH measurements*
The pH values of stained, treated and control (unstained) samples were measured.

Figure 14 shows that both methods have provided satisfying results in the acidity neutralization of the treated photographs. All the samples displayed a reduction of pH values after staining while post treatments the acidity nearly returned to neutral. 25 ml *H. Sabdariffa* recorded the highest of neutralization (6.6) among all the concentrations used in method I. On the other hand, condition IV of method II revealed higher neutralization effect (6.4) than that of condition III (6.1).

*3.2.3 Colorimetric measurement*
The color change was evaluated using the CIE, $L^*a^*b^*$ system because of its convenience for archaeological applications (Carrión-Ruiz *et al.*, 2021; Molada-Tebar *et al.*, 2018).

Data of the three axes were used to obtain the total color difference $\Delta E^*$ using the formula $\Delta E^* = \{(\Delta L^*)2 + (\Delta a^*)2 + (\Delta b^*)2\}^{1/2}$ (Lettieri *et al.*, 2021; Carrión-Ruiz *et al.*, 2021).

The analysis was conducted on stained, treated and control samples.

The results in Table 1 showed that method I achieved satisfied color change values in all treatments. None of the three treatments exceeded the color difference limit ($\Delta E^* = 5$) (Goffredo and Munafò, 2015). In shadow and highlight areas, it was realized that total color change value increased as the

**Figure 12** Digital microscope of F2, F3 and F4 before and after Hs aqueous extract treatments (7, 15 and 25 ml), respectively, compared to control sample

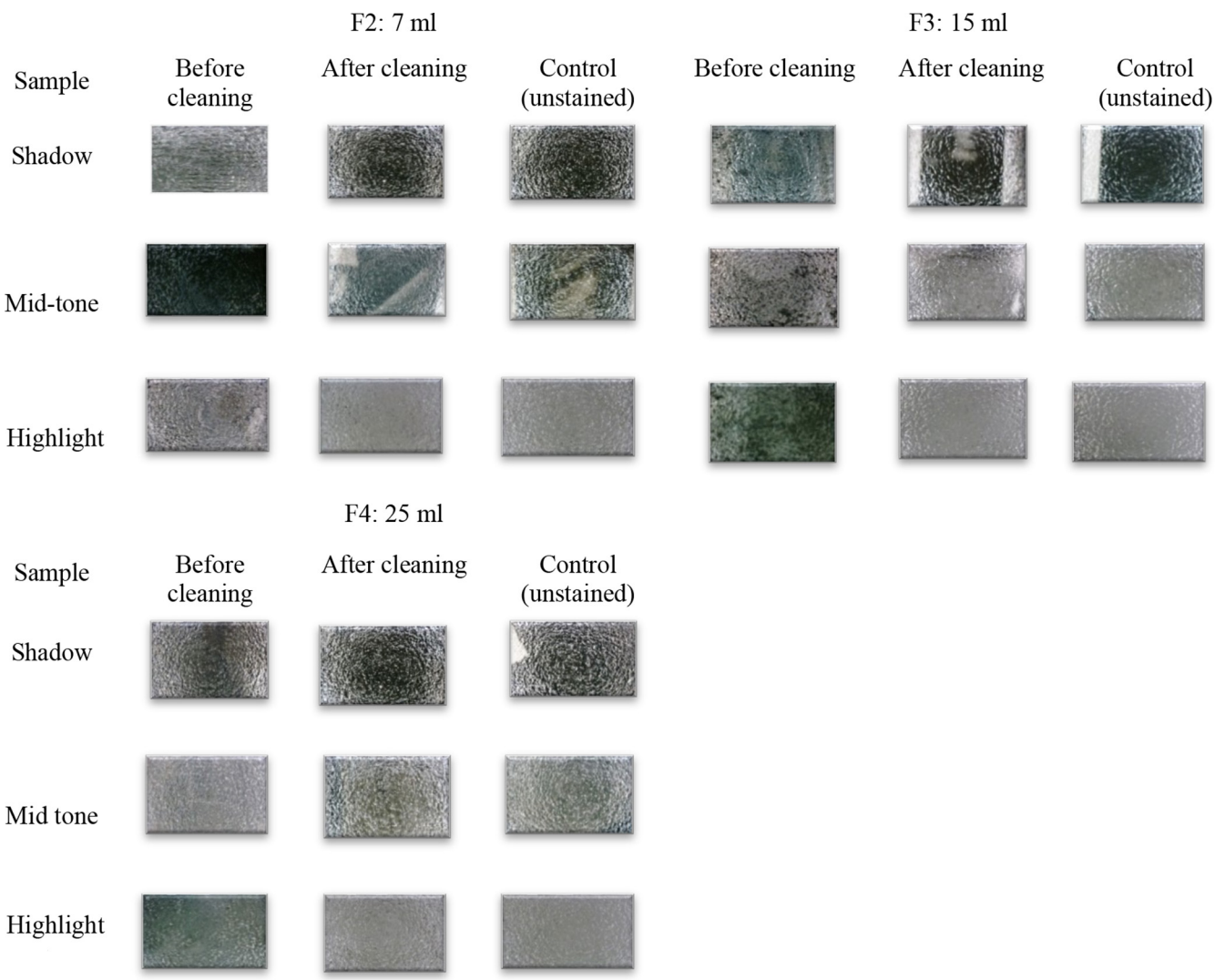

**Figure 13** Digital microscope of plasma in aqueous extract treatments

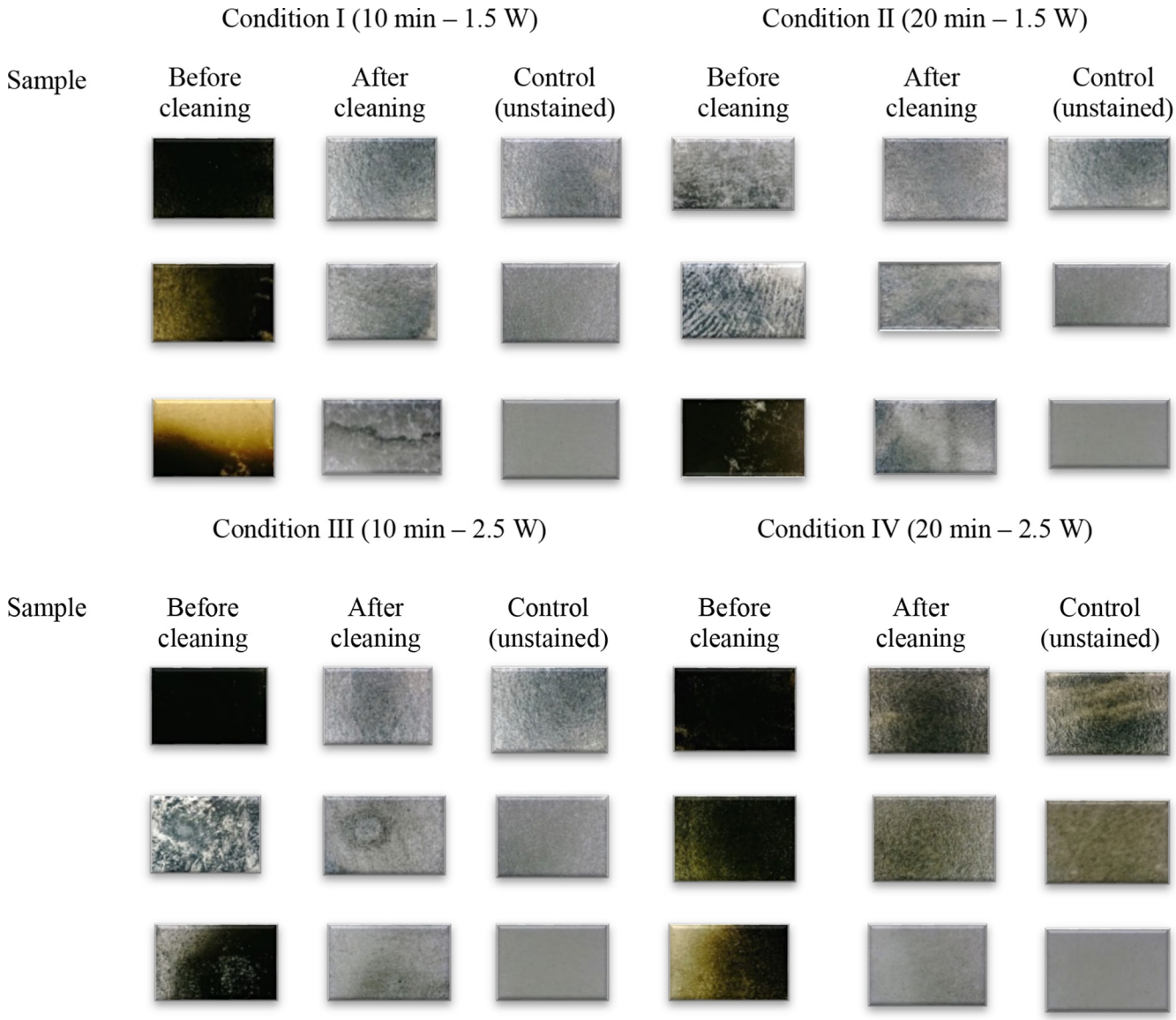


**Figure 14** pH measurements of stained and treated samples compared to unstained samples

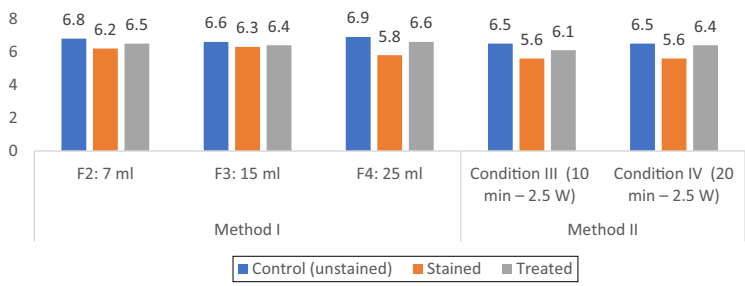


concentration of *H. sabdariffa* increased, i.e. Hs 7 ml treatment exhibited the less $\Delta E^*$ values (0.81, 0.38), respectively. Conversely, in the mid-tone areas, the value of Hs 7 ml was higher ($\Delta E^*$ 1.82) than the $\Delta E^*$ value of Hs 15 ml and Hs 25 ml treatments ($\Delta E^*$ 1.42, 0.71), respectively, while the results in Table 2 showed that in shadow and mid-tone areas, acceptable total color changes were obtained ($\Delta E^* < 5$) after plasma + (Hs) absolute treatment using conditions III and IV. Results of

**Table 1** L*, a*, b* and total color change (ΔE*) values after using method I treatments

| Samples | Method I Hs 7 ml, 15 ml, 25 ml | | | | | | | | | | | |
|---|---|---|---|---|---|---|---|---|---|---|---|---|
| | L* | a* | b* | ΔE* | L* | a* | b* | ΔE* | L* | a* | b* | ΔE* |
| | F2 7 ml (Hs) | | | | F3 15 ml (Hs) | | | | F4 25 ml (Hs) | | | |
| | Shadow area | | | | | | | | | | | |
| **Stained** | 24.79 | 0.38 | 2.95 | 1.90 | 21.39 | 0.28 | 1.26 | 3.57 | 23.63 | 1.87 | 1.82 | 6.50 |
| **Treated** | 22.61 | 0.45 | 4.10 | 0.81 | 23.52 | 0.19 | 2.69 | 1.27 | 27.80 | 0.55 | 5.60 | 1.70 |
| **Control (unstained)** | 23.25 | 0.92 | 3.93 | | 24.76 | 0.15 | 2.44 | | 29.18 | 1.45 | 5.18 | |
| | Mid-tone area | | | | | | | | | | | |
| **Stained** | 22.08 | 0.39 | 1.87 | 17.56 | 28.08 | 0.76 | 4.56 | 10.20 | 29.94 | 1.49 | 5.43 | 23.47 |
| **Treated** | 36.95 | 1.44 | 7.10 | 1.82 | 38.98 | 0.80 | 7.57 | 1.42 | 54.08 | 1.14 | 6.84 | 0.71 |
| **Control (unstained)** | 38.51 | 1.95 | 7.88 | | 38.10 | 0.79 | 6.46 | | 53.37 | 1.07 | 6.81 | |
| | Highlight area | | | | | | | | | | | |
| **Stained** | 35.35 | 2.53 | 7.30 | 44.68 | 49.61 | 2.03 | 6.89 | 32.02 | 52.18 | 2.72 | 12.67 | 26.50 |
| **Treated** | 79.66 | 2.80 | 8.57 | 0.38 | 80.52 | 3.07 | 9.17 | 1.28 | 78.64 | 1.89 | 12.13 | 1.48 |
| **Control (unstained)** | 80.01 | 2.92 | 8.67 | | 81.46 | 3.67 | 9.80 | | 78.65 | 1.96 | 13.61 | |

**Notes:** Satisfied ΔE* values for all method I treatments. None of them exceeded the color difference limit (ΔE* = 5) in all areas

**Table 2** L*, a*, b* and total color change (ΔE*) values after using method II treatments

| Samples | Method II plasma + *H. Sabdariffa* absolute | | | |
|---|---|---|---|---|
| | L* | a* | b* | ΔE* |
| ***Shadow area*** | | | | |
| **Stained** | 19.03 | −0.06 | 0.29 | 6.56 |
| **Control** | 24.49 | 0.76 | 3.83 | |
| **Treated III** | 21.22 | 0.16 | 1.47 | 4.08 |
| **Treated IV** | 22.01 | 0.60 | 2.86 | 2.67 |
| ***Midtone area*** | | | | |
| **Stained** | 23.13 | 0.29 | 1.38 | 14.51 |
| **Control** | 34.34 | 1.58 | 10.50 | |
| **Treated III** | 31.39 | 1.54 | 8.58 | 3.52 |
| **Treated IV** | 33.80 | 1.29 | 9.05 | 1.75 |
| ***Highlight area*** | | | | |
| **Stained** | 28.50 | 2.79 | 8.20 | 58.85 |
| **Control** | 86.23 | 3.42 | 19.60 | |
| **Treated III** | 65.58 | 4.58 | 20.44 | 20.70 |
| **Treated IV** | 70.14 | 4.74 | 21.91 | 16.31 |

**Notes:** Unsatisfied ΔE* values for the method II treatments as both conditions exceeded the color difference limit (ΔE* = 5) in the highlight areas

condition IV were less and more suitable than that of condition IV. On the contrary, in highlight areas, the total color changes indicated that the two plasma conditions induced strong chromatic variations, and the values of conditions III and IV exceeded the limit with values 20.70 and 16.31, respectively.

Based on the previous results, (Hs) 7 ml and condition IV treatments are the most effective treatments.

*3.2.4 Atomic force microscope*

AFM was used to estimate the efficiency of Hs 7 ml extract and condition IV of plasma plus Hs absolute extract cleaning methods on treated samples' surface compared to unstained samples. The analysis depended on measuring roughness parameters that may form dust particles, scratches, etc., on visual surfaces by nanoscale (Henke *et al.*, 2002). The results of roughness average (Ra) and Rms (root-mean-squared-rough) (Rq) were used to determine the achieved extent of cleaning methods and the residues quantities if they existed. Brighter regions defined the higher roughness.

Figure 15 shows the difference between the Ra and Rq of the treated samples and unstained control samples. Method I (Hs 7 ml) treatment revealed approaching roughness to the unstained control samples with Rq (59.61) and Ra (43.24) more than method II (plasma with HS absolute extract) condition IV with Rq (261) and Ra (193.2). Figure 16 displays the 2D and the 3D images of unstained control samples of 7 ml (Hs), which appeared with uniform surface and the 2D and the 3D of treated samples with a less smooth surface. Likewise, in method II 2D, 3D images of unstained control samples viewed smoothed surfaces more than the treated ones. The results may be the residues of the soot post-treatment, which is in accordance with the results of the optical digital microscope investigation. Further study is required in this area. However, in all cases, the change in roughness was mild to moderate.

*3.2.5 Fourier transform infrared-attenuated total reflection analysis*

Infrared absorption spectra of protein showed characteristic absorption bands assigned to the peptide bonds (–CONH–). Amide I is mainly related to the C=O stretching, and it ranges from 1.600 to 1.690 $cm^{-1}$. Amide II, which falls in the 1.480–1.575 $cm^{-1}$ range, is related to the N = H bending and C = N stretching vibration. Amide III ranges from 1.229 to 1.301 $cm^{-1}$ and assignable to CN stretching, NH bending.

These bands are the most used IR spectrum to reveal the conformational changes of the protein (Das *et al.*, 2017). Attenuated total reflection (ATR)-FTIR results in Figure 17 showed approximately no change in positions and transmittance intensities of both amide I and amide II compared to the unstained (control) sample when Hs 7 ml extract was used. While, in case of using plasma + Hs absolute

**Figure 15** Ra and Rq of 7 ml and condition IV treated and control (unstained) samples

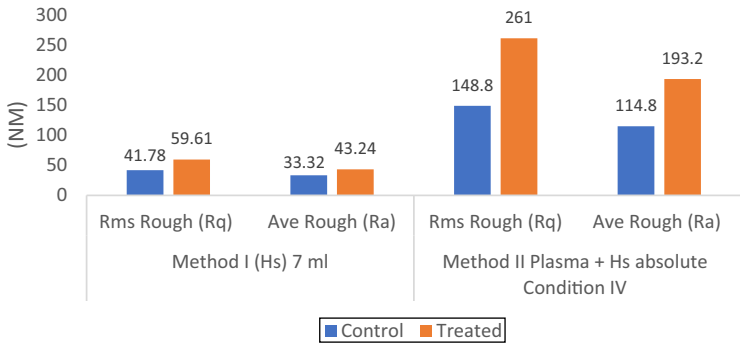


**Figure 16** AFM surface morphology: (a) 3D and 2D of 7 ml (HS) unstained control samples; (b) 3D and 2D of treated samples; (c) 3D and 2D plasma and (HS) absolute extract unstained control samples and (d) 3D and 2D of treated samples

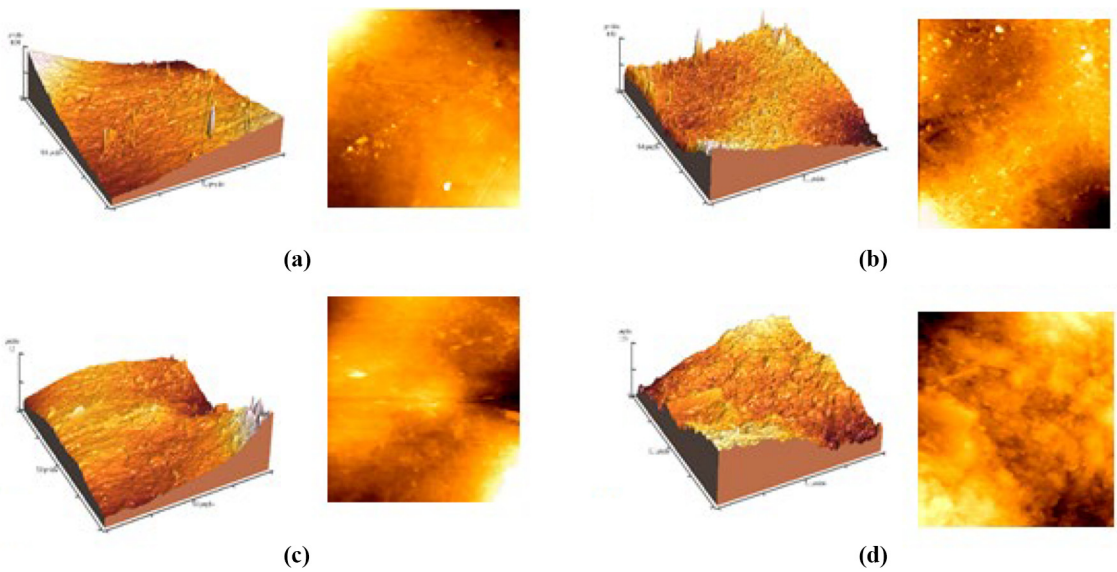


**Figure 17** FTIR-ATR spectra of the samples treated with 7 ml (Hs) and plasma + (Hs) absolute condition IV compared with control samples

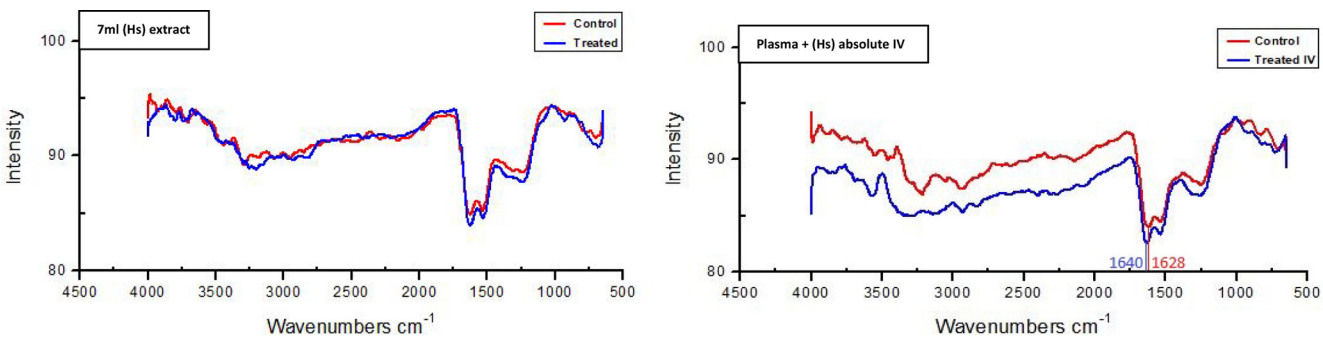


amide I band was shifted to higher frequency (from 1.528 to 1.540 $cm^{-1}$), indicating breakdown of some hydrogen bonding between protein chains. Breakdown of hydrogen bonds decreases crystallinity of protein chains and makes protein more susceptible to chemical reactions and deterioration.

*3.2.6 Mechanical properties*

Tensile strength and elongation percent measurements were conducted on stained, treated and unstained samples. Samples were shaped in stripes shape 15 × 2 cm and were held between two clamps at a fixed distance then pulled at a preset rate.

**Figure 18** Tensile strengths and elongation for samples treated with (Hs) 7 ml and plasma 1 Hs absolute condition IV compared with unstained samples

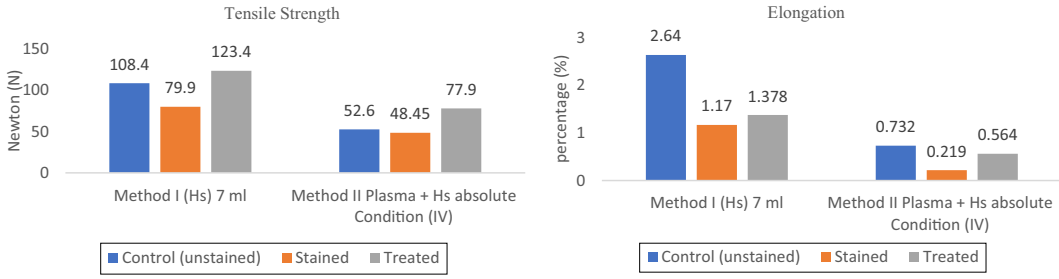


Figure 18 indicates that both methods improved the mechanical properties of the paper support by strengthening the bonds among the cellulose chains. This finding was revealed by improving tensile strength and elongation of the treated samples for both methods. Method I recorded increasing tensile strength value by 40.12% and elongation by 7.88% compared to the stained sample. This increasing is probably as a result of forming hydrogen bonds by the polar groups in the *H. sabdariffa* extract and the free OH groups or the converged hydroxyl groups on the surface of cellulose. On the other hand, crosslinking bonds may be formed between cellulose chains. In contrast, method II revealed superiority in improving the tensile strength by 55.97% and elongation by 47.13%. The surface activation of cellulose following plasma treatments may consist of more free OH groups (unbonded by hydrogen bonds) or the convergence of hydroxyl groups on the surface of cellulose in carbonyl or carboxyl groups or nitrogen containing groups. On the other hand, the intense defibrillation of cellulose promoted by the activation with Ar plasma treatments seem beneficial to the tensile strength and elongation at break of composites containing these celluloses (Vizireanu *et al.*, 2018)

## 4. Conclusion

The paper evaluated the effectiveness of two cleaning methods to remove soot stains from the surface of fire-damaged silver gelatin prints. Therefore, it examined *H. sabdariffa L.* calyces' extract and DBD Ar. plasma combined with the aqueous extract. It showed that lower tested concentrations of *H. sabdariffa L.* calyces' extract efficiently cleaned the surface without causing any stains or damage. Moreover, it provided satisfying results in the acidity neutralization of the treated photographs, the accepted color change values and the improvement of mechanical properties of the treated samples. FTIR results showed approximately no change in bands frequencies and transmittance intensities compared to those of the unstained sample, indicating gelatin's chemical stability post-treatment. On the contrary, plasma in aqueous extract induced strong chromatic variations in highlight areas and made gelatin more susceptible to chemical reactions and deterioration depending on FTIR results.

It is concluded that it is safe to use *H. sabdariffa L.* calyces' extract in cleaning fire-damaged silver gelatin prints more than the plasma with an aqueous extract, which proved to be less effective in cleaning, leaving a light residue of soot and making gelatin more susceptible to deterioration.

## References

Abdel-Aziz, O., Mahmoud, M., Abo-ELfath, Y., Abdel-Aziz, S. and Samir, M.M. (2019), "Evaluation of conventional treatments for mirrored silver gelatin prints: experimental and applied study", *International Journal of Conservation Science*, Vol. 10 No. 1, pp. 81-96.

Abdelghaffar, F., Abdelghaffar, R.A., Rashed, U.M. and Ahmed, H.M. (2020), "Highly effective surface modification using plasma technologies toward green coloration of polyester fabrics", *Environmental Science and Pollution Research*, Vol. 27 No. 23, pp. 28949-28961.

Adochitei, A. and Drochioiu, G. (2011), "Rapid characterization of peptide secondary structure by FT-IR spectroscopy", *Revue Roumaine de Chimie*, Vol. 56 No. 8, pp. 783-791.

Ahmed, H.M., Abd-El Thalouth, J.I., Rashed, U.M. and El-Halwagy, A.A. (2016), "New approach in burn out printing with DBD plasma technique on linen fabric and its blend with polyester", *International Journal of Science and Research (IJSR) ISSN (Online)*, pp. 2319-7064.

Al-Emam, E., Motawea, A.G., Caen, J. and Janssens, K. (2021), "Soot removal from ancient Egyptian complex painted surfaces using a double network gel: empirical tests on the ceiling of the sanctuary of Osiris in the temple of Seti I - Abydos", *Heritage Science*, Vol. 9 No. 1, pp. 1-10.

Ali, M. (2016), "Experimental and applied studies on the effects of selected remedial conservation treatments on the chemical and physical properties of silver gelatin and chromogenic prints", PhD thesis, Faculty of Archaeology, Cairo University, pp. 125-135.

Ali, M., Ali, M., Darwish, S., Saker, U. and Ciliberto, E. (2017), "Solvent cleaning of Antique chromogenic prints: an analytical comparative study", *Mediterranean Archaeology & Archaeometry*, Vol. 17 No. 3, pp. 1-12.

Belkind, A. and Gershman, S. (2008), "Plasma cleaning of surfaces", *Vacuum Coating and Technology,* November, pp. 46-57.

Boselli, M., Chiavari, C., Colombo, V., Gherardi, M., Martini, C. and Rotundo, F. (2017), "Atmospheric pressure non-equilibrium plasma cleaning of 19th century daguerreotypes", *Plasma Processes and Polymers*, Vol. 14 No. 3, p. 1600027.

Carrión-Ruiz, B., Riutort-Mayol, G., Molada-Tebar, A., Lerma, J.L. and Villaverde, V. (2021), "Color degradation mapping of rock art paintings using microfading spectrometry", *Journal of Cultural Heritage*, Vol. 47, p. 103.

Cattò, C., Sanmartín, P., Gulotta, D., Troiano, F. and Cappitelli, F. (2021), "Bioremoval of graffiti using novel commercial strains of bacteria", *Science of the Total Environment*, Vol. 756, p. 144075.

Chawinga, W.D. and Majawa, F. (2018), "An assessment of Mzuzu University library after a fire disaster", *African Journal of Library, Archives & Information Science*, Vol. 28 No. 2, pp. 183-194.

Clarke, C.J., Tu, W.C., Levers, O., Brohl, A. and Hallett, J.P. (2018), "Green and sustainable solvents in chemical processes", *Chemical Reviews*, Vol. 118 No. 2, pp. 747-800.

Da-Costa-Rocha, I., Bonnlaender, B., Sievers, H., Pischel, I. and Heinrich, M. (2014), "*Hibiscus sabdariffa* L. – a phytochemical and pharmacological review", *Food Chemistry*, Vol. 165, pp. 424-443.

Das, M.P., Suguna, P.R., Prasad, K.A.R.P.U.R.A.M., Vijaylakshmi, J.V. and Renuka, M. (2017), "Extraction and characterization of gelatin: a functional biopolymer", *International Journal of Pharmacy and Pharmaceutical Sciences*, Vol. 9 No. 9, pp. 10-22159.

Domingues, J.A., Bonelli, N., Giorgi, R., Fratini, E., Gorel, F. and Baglioni, P. (2013), "Innovative hydrogels based on semi-interpenetrating *p* (HEMA)/PVP networks for the cleaning of water-sensitive cultural heritage artifacts", *Langmuir*, Vol. 29 No. 8, p. 2746.

El-Gohary, M. and Metawa, A. (2016), "Cleaning of architectural bricks using RF plasma. I. metallic stains", *International Journal of Conservation Science*, Vol. 7 No. 3, pp. 669-682.

El-Kinany, R.G., Salama, Y.E., Rozan, M.A., Bayom, H.M. and Nassar, A.M. (2020), "Impacts of humic acid, indole butyric acid (IBA) and arbuscular mycorrhizal fungi (*Glomus mosseae*) as growth promoters on yield and phytochemical characteristics of hibiscus sabdariffa (roselle)", *Alexandria Science Exchange Journal*, Vol. 41 No. 1, pp. 29-41.

Giacometti, A., Campagnolo, L., MacDonald, S., Mahony, S., Robson, T., Weyrich, M., Terras, A. and Gibson, (2016), "Visualizing macroscopic degradation of parchment and writing via multi-spectral images are and conservation of manuscripts 15", *Proceedings of The Fifteenth International seminar held at the University of Copenhagen-gen 2nd-4th April 2014*, Copenhagen, Museum Tusculum Press.

Goffredo, G. and Munafò, P. (2015), "Preservation of historical stone surfaces by TiO2 nanocoatings", *Coatings*, Vol. 5 No. 2, pp. 222-231.

Grieten, E., Schalm, O., Tack, P., Bauters, S., Storme, P., Gauquelin, N. and Schryvers, D. (2017), "Reclaiming the image of daguerreotypes: characterization of the corroded surface before and after atmospheric plasma treatment", *Journal of Cultural Heritage*, Vol. 28, pp. 56-64.

Gupta, V.K. (2019), "Burning libraries: a review through the lens of history", *Journal of Indian Library Association*, Vol. 54 No. 1.

Henke, L., Nagy, N. and Krull, U.J. (2002), "An AFM determination of the effects on surface roughness caused by cleaning of fused silica and glass substrates in the process of optical biosensor preparation", *Biosensors and Bioelectronics*, Vol. 17 Nos 6/7, pp. 547-555.

Hrdlickova Kuckova, S., Crhova Krizkova, M., Pereira, C.L. C., Hynek, R., Lavrova, O., Busani, T. and Sandu, I.C.A. (2014), "Assessment of green cleaning effectiveness on polychrome surfaces by MALDI-TOF mass spectrometry and microscopic imaging", *Microscopy Research and Technique*, Vol. 77 No. 8, pp. 574-585.

Inklebarger, T. (2018), "California libraries in wildfires' wake: paradise, other communities cope with disaster", available at: https://americanlibrariesmagazine.org/blogs/the-scoop/california-libraries-in-wildfires-wake

Ioanid, E.G., Tănase, C., Rusu, D., Vlad, A.M., Cazacu, G., Balaeş, T. and Dunca, S. (2016), "Decontamination effect of radio frequency low-temperature plasma on paper-based materials rev", *Revue Roumaine de Chimie*, Vol. 61 Nos 6/7, p. 58.

Izquierdo-Vega, J.A., Arteaga-Badillo, D.A., Sánchez-Gutiérrez, M., Morales-González, J.A., Vargas-Mendoza, N., Gómez-Aldapa, C.A. and Madrigal-Santillán, E. (2020), "Organic acids from roselle (hibiscus sabdariffa L.) – a brief review of its pharmacological effects", *Biomedicines*, Vol. 8 No. 5, p. 100.

Jamini, T.S., Islam, A.A., Mohi-Ud-Din, M. and Saikat, M.H. (2018), "Phytochemical composition of calyx extract of roselle (*Hibiscus sabdariffa* L.) genotypes", *Journal of Agriculture and Food Sciences*, Vol. 16 No. 1, pp. 13-23.

Lettieri, M., Masieri, M. and Frigione, M. (2021), "Novel nano-filled coatings for the protection of built heritage stonesurfaces", *Nanomaterials*, Vol. 11 No. 2, p. 301.

Maher, S. (2018), "Lightning strike sparks fire at Hopkinton Library", available at: www.nhpr.org/post/lightning-strike-sparks-fire-hopkinton-library (accessed 2 June 2021).

Molada-Tebar, A., Lerma, J.L. and Marqués-Mateu, Á. (2018), "Camera characterization for improving color archaeological documentation", *Color Research & Application*, Vol. 43 No. 1, pp. 47-57.

Naeem, M.A., Zahran, H.A. and Hassanein, M.M. (2019), "Evaluation of green extraction methods on the chemical and nutritional aspects of Roselle seed (*Hibiscus sabdariffa* L.) oil", *OCL*, Vol. 26.

Nieto-Villena, A., Martínez, J.R., de la Cruz-Mendoza, J.A., Valcárcel-Andrés, J.C., Ortega-Zarzosa, G., Solbes-García, Á. and Vázquez-Martínez, E. (2018), "Atomic force microscopy as a tool for binder identification in ancient photographic processes", *Surface and Interface Analysis*, Vol. 50 No. 4, pp. 496-505.

Nordling, L. (2021), "Fire rips through historic South African library and plant unit", *Nature*, Vol. 592 No. 7856, pp. 672-672.

Oravec, M., Haberová, K., Jančovičová, V., Machatová, Z., Čeppan, M. and Huck, C.W. (2019), "Identification of the historic photographic print materials using portable NIR and PCA", *Microchemical Journal*, Vol. 150, p. 104202.

Pianorsi, M.D., Raudino, M., Bonelli, N., Chelazzi, D., Giorgi, R., Fratini, E. and Baglioni, P. (2017), "Organogels for the cleaning of artifacts", *Pure and Applied Chemistry*, Vol. 89 No. 1, p. 4.

Pinela, J., Prieto, M.A., Pereira, E., Jabeur, I., Barreiro, M.F., Barros, L. and Ferreira, I.C. (2019), "Optimization of heat- and ultrasound-assisted extraction of Anthocyanins from *Hibiscus sabdariffa* calyces for natural food colorants", *Food Chemistry*, Vol. 275, pp. 309-321.

Prieto, B., Vázquez-Nion, D., Fuentes, E. and Durán-Román, A.G. (2020), "Response of subaerial biofilms growing on stone-built cultural heritage to changing water regime and $CO_2$ conditions", *International Biodeterioration & Biodegradation*, Vol. 148, p. 104882.

Rebekah, B. (2018), "What happens to smoke damaged books?", available at: https://blogs.k-state.edu/hale/2018/07/17/what-happens-to-smoke-damaged-books/ (accessed 3 June 2021).

Salami, S.O. and Afolayan, A.J. (2020), "Assessment of antimicrobial activities and toxicological effects of green and red cultivars of roselle-*Hibiscus sabdariffa* L", *European Journal of Medicinal Plants*, Vol. 31 No. 15, pp. 11-22.

Sclocchi, M.C., Damiano, E., Matè, D., Colaizzi, P. and Pinzari, F. (2013), "Fungal biosorption of silver particles on 20th-century photographic documents", *International Biodeterioration & Biodegradation*, Vol. 84, pp. 367-371.

Shaheen, R.A., Ali, M.F., Osama Saqr, M., Reda, S.M. and Labeeb, A.M. (2019), "Inquisition on the photochemical degradation of silver gelatin photograph print-out", *J Interv Radiol Nucl Med*, Vol. 2019, pp. 58-66.

Shaheen, R., Fouad, M., Saqr, O., Reda, S. and Labeeb, A. (2020), "Assessment of the photo-chemical degradation of silver gelatin photograph print-out", *International Journal of Conservation Science*, Vol. 11 No. 4.

Stefanova, M. and Kamenarov, Z. (2020), "Using atmospheric pressure plasma as a tool in the cleaning of icon paintings", *IOP Conference Series: Materials Science and Engineering*, IOP Publishing, Vol. 949 No. 1, p. 012087.

Sullivan, M., Brogdon-Grantham, S. and Taira, K. (2014), "*New Approaches to Cleaning Works of Art on Paper and Photographs*, Winterthur/University of DE Program in Art Conservation, ANAGPIC, Newark.

Superio, D.L., Alayon, S.B. and Oliveros, M.G.H. (2019), "Disaster management practices of academic libraries in Panay island, Philippines: lessons from typhoon Haiyan", *Information Development*, Vol. 35 No. 1, pp. 51-66.

Tinõ, R., Vizárová, K. and Krčma, F. (2019), "Plasma surface cleaning of cultural heritage objects", *Nanotechnologies and Nanomaterials for Diagnostic, Conservation and Restoration of Cultural Heritage*, Elsevier, pp. 239-275.

Tomšová, K. and Ďurovič, M. (2017), "Influence of disinfection methods on the stability of black and white silver gelatin prints", *Journal of Cultural Heritage*, Vol. 24, pp. 78-85.

Turvey-Welch, M.R. and Talbot, K. (2018), "Trial by fire, water, and soot: Kansas State University's collection disaster plan dissected and what you can learn from our disaster", *KS Library Association/Mountain Plains Library Association* pp. 60-70.

Vizireanu, S., Panaitescu, D.M., Nicolae, C.A., Frone, A.N., Chiulan, I., Ionita, M.D., Satulu, V., Carpen, L.G., Petrescu, S., Birjega, R. and Dinescu, G. (2018), "Cellulose defibrillation and functionalization by plasma in liquid treatment", *Scientific Reports*, Vol. 8 No. 1, pp. 1-14.

Volpi, F. (2017), "Green strategies for the cleaning of works of art setting up of an analytical protocol for the evaluation of cleaning", Doctoral dissertation, ALMA, p. 9.

Yosri, A., Mohamed, N., Atef, A., Atef, O. and Attia, R.A.M. (2020), "Analytical study on the effect of pollutants on silver gelatin prints", *International Journal of Conservation Science*, Vol. 11 No. 1, pp. 39-50.

Zachariášová, B., Haberová, K., Oravec, M. and Jančovičová, I.V. (2019), "Plasma treatment of gelatin photography", *Acta Chimica Slovaca*, Vol. 12 No. 1, pp. 27-33.

## Corresponding author

**Laila M. Elattar** can be contacted at: Lailaelattar@ymail.com